Eosinophil-Granule Major Basic Protein, a C-Type Lectin, Binds Heparin[†,‡]

G. Jawahar Swaminathan,[§,||] David G. Myszka,[⊥] Phinikoula S. Katsamba,[⊥] Lyo E. Ohnuki,[#] Gerald J. Gleich,[#,@] and K. Ravi Acharya*[,§]

Department of Biology and Biochemistry, University of Bath, Claverton Down, Bath BA2 7AY, United Kingdom, and Center for Biomolecular Interaction Analysis and Departments of Dermatology and Medicine, University of Utah School of Medicine, Salt Lake City, Utah 84132-2409

Received June 10, 2005; Revised Manuscript Received September 2, 2005

ABSTRACT: The eosinophil major basic protein (EMBP), a constituent of the eosinophil secondary granule, is implicated in cytotoxicity and mediation of allergic disorders such as asthma. It is a member of the C-type lectin family, but lacks a Ca^{2+}- and carbohydrate-binding site as seen in other members of this family. Here, we report the crystal structure of EMBP in complex with a heparin disaccharide and in the absence of Ca^{2+}, the first such report of any C-lectin with this sugar. We also provide direct evidence of binding of EMBP to heparin and heparin disaccharide by surface plasmon resonance. We propose that the sugars recognized by EMBP are likely to be proteoglycans such as heparin, leading to new interpretations for EMBP function.

The eosinophil major basic protein (EMBP)[1] is the most abundant constituent of the eosinophil secondary granule, forming its crystalloid core. EMBP activities include cytotoxicity toward bacteria and mammalian cells in vitro and helminthotoxicity (*1*). The level of EMBP is elevated in biological fluids from patients with asthma and other eosinophil-associated diseases (*2*). EMBP also causes release of histamine from mast cells and basophils, activates neutrophils and alveolar macrophages, and is directly implicated in epithelial cell damage, exfoliation, and bronchospasm in allergic diseases such as asthma (*3*−*6*). EMBP (pI = 11.4) appears to damage cells by virtue of disrupting the bilayer lipid membrane (*7*) or altering the activity of enzymes within tissues (*8*). We have previously reported the structure of native EMBP (*9*). EMBP is structurally related to members of the animal C-type lectin (C-TL) family but exhibits significant differences in the carbohydrate-recognition site, in both sequence and structure. We predicted that the mode of carbohydrate recognition and the sugars recognized by EMBP were likely to be very different from those observed for other C-TLs.

Here we report the crystal structure of EMBP in complex with a heparin disaccharide (HD) at a resolution of 2.2 Å. The EMBP heparin binding site is similar to the carbohydrate-binding site seen in other C-TLs. However, heparin recognition by EMBP does not involve Ca^{2+} coordination. In addition, we report the strength of binding of heparin to the EMBP molecule using surface plasmon resonance. Our detailed analyses show that the natural carbohydrate ligands for EMBP are likely to be long chain proteoglycans with which proteoglycan cores are substituted (like heparin).

EXPERIMENTAL PROCEDURES

Protein Purification, Crystallization, and Soaking. EMBP was purified from eosinophil granules of patients with marked eosinophilia essentially as described previously (*10*, *11*). The crystallization conditions for EMBP have been described previously (*9*). EMBP crystals were soaked with a 5 mM solution (final concentration) of heparin disaccharide I-S (Sigma Chemical Co., catalog number H-9267), for a period of 30 min prior to data collection.

Diffraction Measurements and Structure Determination. Diffraction data to a resolution of 2.2 Å for flash-frozen crystals were collected on station PX14.1 at the Synchrotron Radiation Source (Daresbury, U.K.) using an ADSC Quantum-4 CCD detector. Raw data images were indexed and scaled using the DENZO and SCALEPACK modules of the HKL Suite (*12*) (Table 1). The structure of the EMBP−heparin disaccharide (EMBP−HD) complex was determined by the molecular replacement method using the native EMBP structure monomer (PDB entry 1H8U) (*9*) as the starting search model.

Refinement of the EMBP−HD complex structure was performed using CNS (*13*), with 5% of the reflections excluded for calculation of the cross-validated *R*-factor (R_{free}). After the first round of refinement, clear density corresponding to the heparin disaccharide could be seen in sigmaA

[†] This work is supported by the Wellcome Trust (UK) through a Programme Grant (067288) to K.R.A. and National Institutes of Health Grant AI 09728 to G.J.G.

[‡] The atomic coordinates and structure factors (entries 2BRS and R2BRSSF, respectively) have been deposited in the Protein Data Bank.

* To whom correspondence should be addressed. Phone: +44-1225-386238. Fax: +44-1225-386779. E-mail: bsskra@bath.ac.uk.

[§] University of Bath.

[||] Present address: European Bioinformatics Institute, Wellcome Trust Genome Campus, Hinxton, Cambridge CB10 1XD, United Kingdom.

[⊥] Center for Biomolecular Interaction Analysis, University of Utah School of Medicine.

[#] Department of Dermatology, University of Utah School of Medicine.

[@] Department of Medicine, University of Utah School of Medicine.

[1] Abbreviations: EMBP, eosinophil major basic protein; C-TL, C-type lectin; HD, heparin disaccharide.

10.1021/bi051112b CCC: $30.25
Published on Web 10/07/2005

Table 1: Statistics for Data Collection and Refinement

wavelength (Å)	1.488
resolution range (Å)	40−2.2
space group	*C*2
no. of observations	162812
no. of unique reflections	12698
R_{sym} (%)[a] (outermost shell)[b]	9.4 (34.1)
completeness (%) (outermost shell)[b]	99.5 (98.3)
$I/\sigma I$ (outermost shell)[b]	10.5 (2.5)
crystallographic *R*-factor (%) (R_{cryst})[c]	24.7
R_{free} (%) (R_{free})[d]	29.1
deviations from ideality	
bond lengths (Å)	0.007
bond angles (deg)	1.40
B-factor statistics (Å^2)	
overall *B*-factor	28.69
protein atoms (1920 total)	
main chain	27.45
side chain	28.03
solvent atoms (92 in total)	31.92
sulfate ions (40 atoms in total)	49.90
heparin disaccharide (35 in total)	48.08

[a] $R_{sym} = \sum_h\sum_i[|I_i(h) - \langle I(h)\rangle|/\sum_h\sum_i I_i(h)]$, where I_i is the *i*th measurement and $\langle I(h)\rangle$ is the weighted mean of all measurements of $I(h)$. [b] The outermost shell is from 2.28 to 2.20 Å. [c] $R_{cryst} = \sum_h|F_o - F_c|/\sum hF_o$, where F_o and F_c are the observed and calculated structure factor amplitudes, respectively, of reflection *h*. [d] R_{free} is equal to R_{cryst} for a randomly selected 5% subset of reflections that are not used in refinement.

weighted difference maps. The sugar was incorporated in the next cycle of refinement. Water molecules were included at this stage if they had peak heights of $>3\sigma$ in $F_o - F_c$ difference electron density maps and were within hydrogen bonding distance of appropriate atoms. Eight molecules of sulfate ion were also identified in the structure and were included in the final stages of refinement.

The final model of the EMBP−HD complex comprises residues 3−117 for both molecules in the asymmetric unit and has a crystallographic *R*-factor of 24.7% and an R_{free} of 29.1% (Table 1). All the residues of the dimer lie in accepted regions of the Ramachandran ($\phi-\psi$) map, with 91% of the residues in the most favorable regions. No side chain electron density could be seen for residues 46, 47, and 49 in either molecule and were modeled as alanines in the final structure. As the heparin disaccharide was bound to only one molecule of EMBP in the asymmetric unit, only this molecule has been described in detail.

EMBP Ligand Binding Screen. Binding of ligands to EMBP in a screening mode was performed using a Biacore 2000 instrument (Biacore Inc., Piscataway, NJ), equipped with a CM4 sensor chip (Biacore Inc.). HBS [10 mM HEPES (pH 7.4) and 150 mM NaCl] was used as the running buffer. EMBP was immobilized to the sensor surfaces using thiol coupling chemistry. Immobilizations were performed at 37 °C in HBS. All four surfaces were activated using 0.4 M PDEA [2-(2-pyridinyldithio)ethaneamine, Biacore Inc.], prepared in 0.1 M MES (pH 5.0), mixed with an equal volume of 0.1 M EDC [*N*-ethyl-*N*′-(3-dimethylaminopropyl)carbodiimide hydrochloride], and injected for 7 min at a flow rate of 20 μL/min. EMBP was prepared in sodium acetate (pH 5.25) at a concentration of 0.6 μM and injected over the surface for 1 min at a flow rate of 20 μL/min, resulting in an immobilization level of 1300 RU of protein. Binding of the EMBP ligands was tested at 20 °C in HBS running buffer. Six ligands were prepared at a concentration of 12 nM each to rank their binding to EMBP. All ligands were obtained from Sigma with the exception of chondroitin sulfate C, which was obtained from MP Biomedicals. Ligands are as follows, with molecular mass estimates as indicated: heparin from porcine intestinal mucosa, 18 kDa, catalog number H-3393; hyaluronic acid from human umbilical cord, 4500 kDa, catalog number H-1876; mucin I-S from bovine submaxillary glands, 400 kDa, catalog number M-3895; heparan sulfate from bovine kidney, 11 kDa, catalog number H-7640; chondroitin sulfate B from porcine intestinal mucosa, 30 kDa, catalog number C-3788; and chondroitin sulfate C from shark cartilage, 60 kDa, catalog number 970551. Samples were injected for 10 min each at a flow rate of 25 μL/min followed by a 40 min dissociation phase. Regeneration of the EMBP surface was achieved using two 5 s pulses of 6 M guanidine-HCl at 100 μL/min. Each concentration was injected over the surface in triplicate. An empty flow cell served as a reference surface to remove systematic noise from the binding responses. Buffer injections were performed throughout the experiment for double-referencing analysis. The binding responses were normalized for the molecular mass of each GAG tested and then adjusted for the maximum response of the best binder, heparin.

Binding Analysis of Disaccharides Interacting with EMBP. The binding of disaccharides to EMBP was investigated using an S51 biosensor (Biacore Inc.). A CM4 sensor chip was utilized for immobilization of EMBP using HBS as the running buffer. EMBP immobilization was performed using thiol chemistry as described in the screening section. Both the EMBP and reference spots were derivatized using PDEA, but EMBP was immobilized over spot 1 only by injecting it for 7 min at a flow rate of 10 μL/min, resulting in an immobilization level of 3800 RU. Binding was tested at 25 °C using HBS buffer as the running buffer. A total of nine disaccharides were prepared in running buffer and tested for binding using a 2-fold concentration series ranging from 750 to 11.5 μM. All disaccharides were obtained from Sigma: heparin disaccharide I-S, catalog number H-9267; hyaluronic acid disaccharide δDi-HA, catalog number H-9649; chondroitin disaccharide Δdi-6S, catalog number C-4170; D-(+)-cellobiose, catalog number C-7252; D-(+)-trehalose, catalog number T-9531; and disaccharide kit containing maltose, sucrose, isomaltose, and α-lactose, catalog number 47268U. For each sample, a 20 μL volume was injected at a flow rate of 90 μL/min. At the end of the injection, the disaccharides dissociated back to baseline, eliminating the need for a regeneration step. As in the screening assay, injections were performed in triplicate with buffer injections dispersed throughout the assay for double referencing of the data.

RESULTS

Quality of the EMBP−HD Structure. The structure of the EMBP−HD complex is similar to that seen in the 1.8 Å native structure (*9*) (Figure 1A). There are two molecules of EMBP in the asymmetric unit. The EMBP complex structure has an rms deviation of 0.39 Å over 228 Cα atoms compared with the native structure with most variation arising from the flexible loop of residues 45−50 that was not well defined in the native structure as well. The presence of the heparin disaccharide was identified by analysis of the sigmaA weighted difference electron density maps contoured at 3σ (Figure 2A). The final structure has values for the crystal-

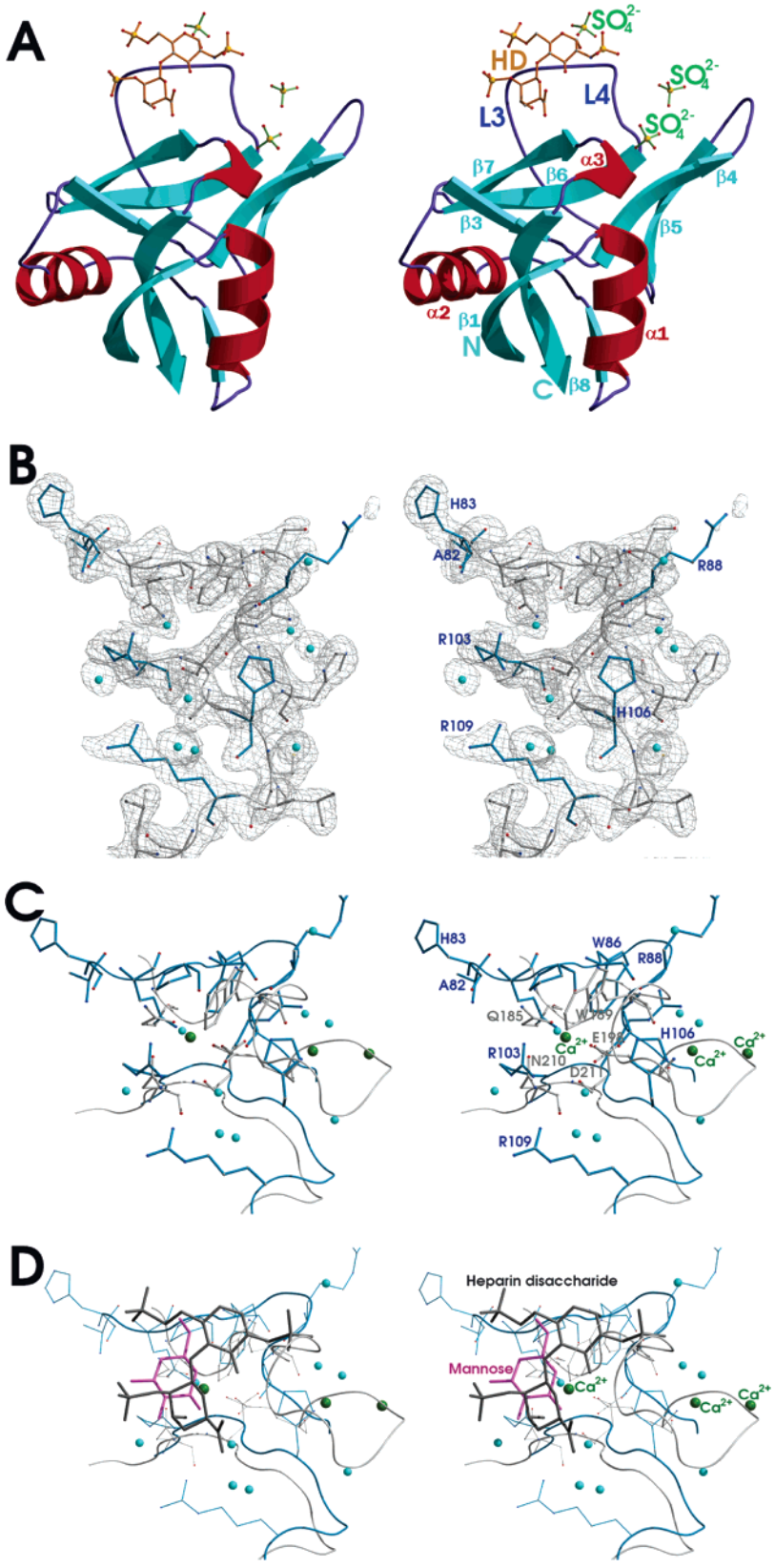

FIGURE 1: (A) Stereoview showing the overall structure of EMBP in complex with heparin disaccharide (HD). The bound sugar is shown in ball-and-stick representation, and the bound sulfate ions are shown as bonds. (B) Portion of the $2F_o - F_c$ electron density map (contoured at the 1σ level) for the carbohydrate-binding site (the lost calcium binding site replaced with a water molecule) in EMBP−HD. Bound water molecules are shown as blue spheres. Hydrogen bonding residues with HD are colored blue. For clarity, the bound HD is not shown. (C) Superposition of the residues that make up the carbohydrate-binding site in EMBP (blue) and from MBP (PDB entry 1AFA) (gray). Calcium ions from MBP are shown as green spheres. Bound water molecules from the EMBP−HD complex are shown as blue spheres. (D) Superposition of the carbohydrate-binding site of EMBP (blue) in complex with HD (black) with that seen in MBP (gray) in complex with mannose (pink). Bound water molecules from the EMBP−HD complex are shown as blue spheres. All pictures were made using BOBSCRIPT (*36*) unless otherwise indicated.

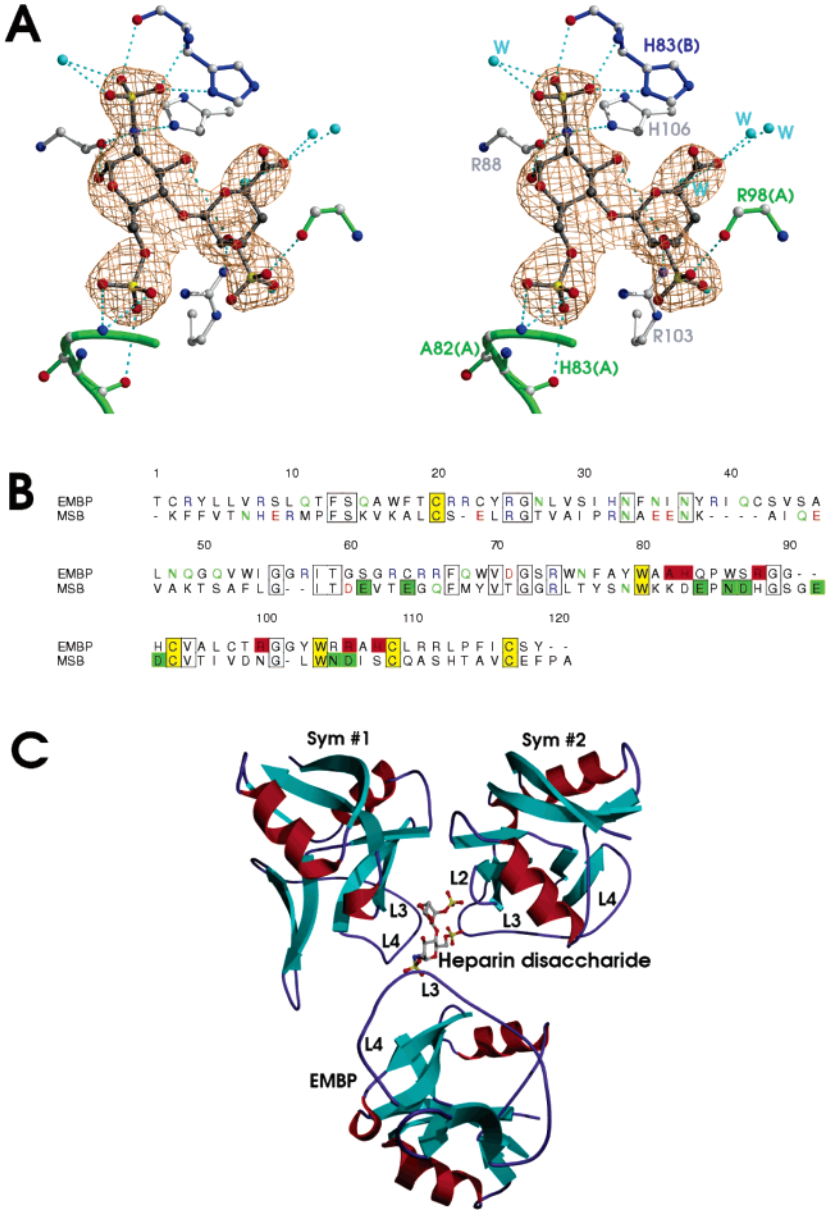

FIGURE 2: (A) Stereoview showing the interaction of heparin disaccharide with EMBP. The sugar is superimposed with a $2F_o - F_c$ difference electron density map contoured at the 1σ level (brick); hydrogen bond contacts are shown as dashed lines, solvent atoms colored cyan, and symmetry-related molecules colored green and blue, respectively. (B) Nature of the carbohydrate-binding site highlighted by sequence comparisons between EMBP and MBP. Residues involved in heparin binding in EMBP (red background) are analogous in position to residues involved in MBP sugar recognition (green background) and Ca^{2+} recognition (green background, boxed). All identical residues are boxed with those defining the C-lectin fold in yellow. All charged residues are shown as basic (blue) or acidic (light green). This figure was produced by ALSCRIPT (*37*). (C) Interactions of a single molecule of heparin disaccharide with two symmetry molecules of EMBP in the crystal. The loops which interact with each molecule of EMBP are highlighted.

lographic *R*-factor and cross-validated *R*-factor of 24.7 and 29.1%, respectively. The overall *B*-factor of the sugar (48.1 Å^2) compares well with the average *B*-factor of the EMBP residues in the neighborhood of the sugar (44.3 Å^2).

Mode of EMBP Carbohydrate Recognition. The heparin binding site of EMBP is situated at the top of the molecule (Figure 1A) and made up of residues from long loops L3 and L4 and strand β7 and comprises residues in the range of 82−106 of EMBP. The local architecture of the protein is stabilized by a disulfide bond (Cys92−Cys107) which links the β-sheet formed by β3, β6, and β7 with the opposite face of the molecule (Figure 1A). The HD was found to bind to EMBP by formation of hydrogen bond interactions with Arg88, Arg103, and His106 (Figure 2A). In addition to these residues from the carbohydrate-binding site, four water molecules near the binding site provide additional hydrogen bond interactions with the sugar moiety, thereby increasing the binding affinity for the disaccharide in this complex. Interestingly, two symmetry-related molecules near the carbohydrate-binding site also provide residues that form potential hydrogen bonds with the sugar (Table 2). Therefore, each molecule of HD is in contact with three molecules of EMBP in the crystal structure. The molecules of EMBP are arranged around a pseudo-3-fold axis with HD at the apex (Figure 2C). Furthermore, the regions of these symmetry-related molecules that interact with the sugar are also from the regions that correspond to loops L3 and L4 of those molecules. Numerous van der Waals contacts between the sugar moiety and EMBP provide additional stability for the heparin disaccharide with EMBP. The ability of multiple

Table 2: Hydrogen Bonding Interactions between EMBP and Heparin Disaccharide

protein atom[a]	solvent atom	carbohydrate atom	distance (Å)
Arg103 Nη2	–	O3	2.44
	Wat5 OH2	O2S	2.75
	Wat60 OH2	O61	3.03
	Wat88 OH2	O61	2.75
	Wat4 OH2	O61	3.08
Arg88 O	–	N	3.14
Arg88 O	–	O1	3.23
His106 Nϵ2	–	O1S	3.37
	Wat35 OH2	O2S	3.28
	Wat35 OH2	O1S	2.85
^{A}His83 Nδ1	–	O3S	2.96
^{A}His83 N	–	O3S	2.74
^{A}His83 N	–	O2S	3.01
^{B}Ala82 N	–	O6S	3.13
^{B}Ala82 N	–	O5S	3.19
^{B}His83 O	–	O4S	3.34
^{B}Arg98 O	–	O1S	2.50

[a] Superscript letters A and B indicate residues from two symmetry-related molecules of EMBP.

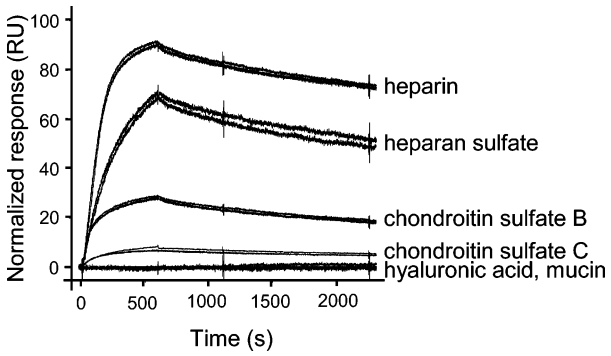

FIGURE 3: Binding of GAGs to EMBP studied by surface plasmon resonance. Six GAGs were screened for binding to immobilized EMBP. The binding responses that are shown are normalized to account for differences in the molecular mass of the different GAGs tested and adjusted for the maximum response of the best binder, heparin. Mucin and hyaluronic acid did not interact with EMBP at 12 nM, as shown by the overlaying baseline signals.

molecules of EMBP to interact with a single molecule of HD suggests a possible mechanism for explaining the observed effects of aggregation and multimerization of EMBP molecules in a solution containing heparin.

Preferential Binding of Heparin by EMBP. To test the affinity and specificity of binding of heparin by EMBP, the binding affinities of several different glycosaminoglycans (GAGs) were examined by surface plasmon resonance (Figure 3). Six different GAGs were passed over the EMBP surface and their binding responses ranked. Heparin demonstrated the greatest binding response of the six GAGs that were tested, with heparan sulfate also demonstrating a high affinity for EMBP. Chondroitin sulfate B exhibited medium-affinity binding; chondroitin sulfate C had low-affinity binding, and mucin and hyaluronic acid did not bind.

To further investigate these binding responses, interactions between disaccharides and EMBP were examined (Figure 4). Nine disaccharides were tested, with binding demonstrated by heparin, chondroitin sulfate, and hyaluronic acid. The binding responses of these were weak yet reproducible, and concentration-dependent, reaching equilibrium rapidly followed by a fast dissociation at the end of the injection. The remaining six disaccharides, α-lactose monohydrate,

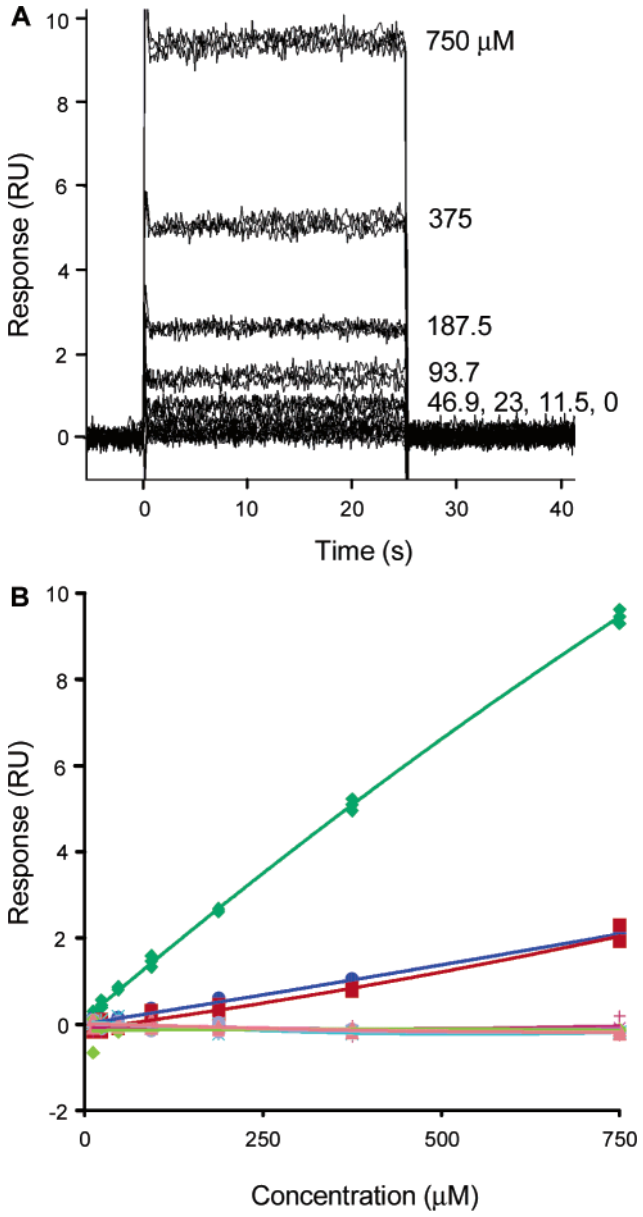

FIGURE 4: Binding of dissacharides to EMBP studied by surface plasmon resonance. Panel A shows the binding of the heparin disaccharide to immobilized EMBP. Heparin disaccharide was injected at concentrations ranging from 750 to 11.5 μM. Injections were performed for 25 s at a flow rate of 90 mL/min. Panel B shows a plot of the binding responses for the nine disaccharides tested against the concentration. The results for heparin, chondroitin sulfate, and hyaluronic acid disaccharides are depicted with diamonds, circles, and squares, respectively. The flat lines represent the responses of six negative controls tested, α-lactase monohydrate, maltose monohydrate, sucrose, isomaltose, trahalose trihydrate, and cellobiose.

maltose monohydrate, sucrose, isomaltose, trehalose trihydrate, and cellobiose, did not demonstrate any binding to the EMBP surface. Binding was not detected over the control surface, indicating the specificity of the three disaccharides for EMBP.

EMBP: A Unique Member of the CT-L Family. The topology of EMBP is similar to that of canonical C-TL domains, which include rat mannose-binding protein (MBP) (*14*), E-selectin (ESL) (*15*), and lung surfactant protein (SP-D) (*16*). It also resembles the C-TL domain-like structures from the CD94 subunit of the natural killer cell receptor

(CD94/NKG2) (*17*), the C-TL domain from the human hematopoietic cell receptor CD69 (*18*, *19*), and the link module from ovulation- and inflammation-associated protein TSG-6 (*20*). The overall deviation between EMBP and the lectin cores of other C-TL family members is between 1.2 and 1.6 Å over 90−103 Cα atoms, with 1.28 Å for the archetype member, MBP (PDB entry 2MSB).

Calcium recognition is a prerequisite for carbohydrate recognition in all the canonical C-TLs (*21*, *22*). The Ca^{2+}- and carbohydrate-binding sites are overlapping in these proteins with at least one distinct, highly conserved site made up by loops L3 and L4 and a β-strand analogous to β7 in EMBP (Figure 1C). The structures of a few C-TLs have been determined in complex with sugar molecules, but none in complex with sulfated sugars such as heparin (*23*, *24*). In all these proteins, binding of the carbohydrate involves the formation of a Ca^{2+} ion-coordinated nucleus with binding specificity provided by conserved pairs of acidic residues. In MBP, these residues are Glu161, Glu165, Glu185, Asn187, Asp188, Glu193, Asp194, Asn203, and Asp205. Some of these residues are involved in coordination with the metal ion, while others provide hydrogen bonding interactions with the sugar molecule. In EMBP, there are no acidic residues save for Asp71 that is not present near the carbohydrate-binding site. Instead, the residues that are present in the sugar-binding site are Ala82, His83, Arg88, His91, Arg98, Arg103, Arg104, and His106 (Figures 1C and 2B). These changes effectively abolish the ability of EMBP to coordinate calcium (replaced by a water molecule, Figure 1B,C) by reversing charge in the binding site and thereby preclude carbohydrate recognition in this manner. However, the binding pocket seems to be most favorable for binding an anionic disaccharide such as heparin disaccharide (Figure 1D). The ability of EMBP to specifically bind heparin suggests that it is a unique member of the C-TL family in terms of its ability to recognize sulfated sugars such as heparin in a Ca^{2+}-independent manner.

DISCUSSION

Lectins are involved in cell surface sugar recognition in bacteria, animals, and plants. Their roles include mediation of cell−cell interactions, pathogen neutralization, and uptake of glycoconjugates (*25*). In animals, the C-TLs are involved in both pathogen recognition and cellular interactions that lead to pathogen neutralization. Among the family of C-TLs, the serum mannose-binding proteins (MBPs) mediate the elimination of infecting pathogens by activation of the complement pathway. The ability of EMBP to specifically and irreversibly bind to heparin without having any appreciable affinity toward mannose has been demonstrated previously (*9*). Our work demonstrates that the heparin binding site of EMBP is analogous to the Ca^{2+}- and carbohydrate-binding site in other C-TLs and not an artifact of protein basicity. In addition, surface plasmon resonance showed that EMBP preferentially binds to heparin as demonstrated by interaction with glycosaminoglycans as well as their disaccharides (Figures 3 and 4).

EMBP function can be neutralized by the addition of heparin into experimental setups both in vivo and in vitro (*26*−*28*). EMBP is toxic toward parasites and causes damage to schistosomula of *Schistosoma mansoni* by disruption of the membrane, an activity that can be inhibited by heparin (*29*). The outer membrane of these parasites is rich in *N*-glycans and proteoglycans such as dermatan sulfate (*30*). Biochemical analysis of EMBP on synthetic lipid bilayers has demonstrated that the likely mode of its toxicity is due to association with anionically charged membrane surfaces, causing membrane depolarization by its high basic charge and disrupting membrane integrity (*7*). EMBP causes ciliostasis and exfoliation of respiratory epithelial cells, an effect similar to the pathology of asthma (*31*, *32*). EMBP does not cause bronchial hyperreactivity in airway smooth muscle rings where the epithelium had been removed but, when epithelium is intact, shows marked reactivity to stimulation by histamine and acetylcholine (*33*). Long chain proteoglycans are found on the surfaces of most epithelial cells and are involved in the mediation of cell−cell communication. The respiratory epithelial cells and basal membranes in the lung are also rich in proteoglycans. Cultured alveolar epithelial cells produce perlecan and collagen XV, both proteoglycans, among other constituents of the basal membrane (*34*, *35*). These results suggest that alveolar epithelial cells could serve as potential targets for EMBP function in tissue damage during inflammation. The existence of analogous yet different binding sites on EMBP molecules as seen in the interaction of HD with symmetry-related molecules suggests a possible mode by which long chain heparin molecules or proteoglycans on the surface of epithelial cells could cause aggregation of EMBP molecules on their surface, leading to observed effects (Figure 2C).

CONCLUSION

We have demonstrated that EMBP is a unique member of the C-TL family that recognizes heparin in a manner that does not require the presence of Ca^{2+} coordination. The binding of HD in a region analogous to the CRD of other C-TLs suggests that the heparin−EMBP interaction is specific and not due to its basicity. These studies provide a better understanding of the mechanisms that would probably dictate EMBP activity in the cell, and provide a platform from where further studies toward developing therapeutics may be undertaken.

The ability of EMBP to bind heparin-like sugars, coupled with its highly basic nature, can be used to explain most of the observed activities of EMBP, particularly its ability to cause membrane disruption, exfoliation, and cytotoxicity. We speculate that EMBP action involves a two-step process. Following release from the granule, EMBP binds to membranes via its ability to recognize proteoglycans on the surface, forming large cross-linked insoluble aggregates. The second step involves cell lysis caused by the depolarization of the plasma membrane by large numbers of EMBP molecules on the surface. Similarly, activation of mast cells and basophils can be hypothesized to occur by the binding of EMBP to cell receptors, their possible dimerization unleashing a cascade of events that ultimately lead to allergic symptoms such as asthma.

ACKNOWLEDGMENT

We thank the scientists at the Synchrotron Radiation Source, Daresbury (U.K.) for their help with X-ray data

collection and Nethaji Thiyagarajan and Matthew Baker for their help during the preparation of the manuscript.

REFERENCES

1. Gleich, G. J., Jacoby, D. B., and Fryer, A. D. (1995) Eosinophil-associated inflammation in bronchial-asthma: A connection to the nervous system, *Int. Arch. Allergy Immunol. 107*, 205−207.
2. Wassom, D. L., Loegering, D. A., Solley, G. O., Moore, S. B., Schooley, R. T., Fauci, A. S., and Gleich, G. J. (1981) Elevated serum levels of the eosinophil granule major basic-protein in patients with eosinophilia, *J. Clin. Invest. 67*, 651−661.
3. Gleich, G. J., Frigas, E., Loegering, D. A., Wassom, D. L., and Steinmuller, D. (1979) Cytotoxic properties of the eosinophil major basic protein, *J. Immunol. 123*, 2925−2927.
4. Gleich, G. J (2000) Mechanisms of eosinophil-associated inflammation, *J. Allergy Clin. Immunol. 105*, 651−663.
5. Piliponsky, A. M., Pickholtz, D., Gleich, G. J., and Levi-Schaffer, F. (2001) Human eosinophils induce histamine release from antigen-activated rat peritoneal mast cells: A possible role for mast cells in late-phase allergic reactions, *J. Allergy Clin. Immunol. 107*, 993−1000.
6. Moy, J. N., Gleich, G. J., and Thomas, L. L. (1990) Noncytotoxic activation of neutrophils by eosinophil granule major basic-protein: Effect on superoxide anion generation and lysosomal-enzyme release, *J. Immunol. 145*, 2626−2632.
7. Abu-Ghazaleh, R. I., Gleich, G. J., and Prendergast, F. G. (1992) Interaction of eosinophil granule major basic-protein with synthetic lipid bilayers: A mechanism for toxicity, *J. Membr. Biol. 128*, 153−164.
8. Hastie, A. T., Loegering, D. A., Gleich, G. J., and Kueppers, F. (1987) The effect of purified human eosinophil major basic protein on mammalian ciliary activity, *Am. Rev. Respir. Dis. 135*, 848−853.
9. Swaminathan, G. J., Weaver, A. J., Loegering, D. A., Checkel, J. L., Leonidas, D. D., Gleich, G. J., and Acharya, K. R. (2001) Crystal structure of the eosinophil major basic protein at 1.8 Å: An atypical lectin with a paradigm shift in specificity, *J. Biol. Chem. 276*, 26197−26203.
10. Abu-Ghazaleh, R. I., Dunnette, S. L., Loegering, D. A., Checkel, J. L., Kita, H., Thomas, L. L., and Gleich, G. J. (1992) Eosinophil granule proteins in peripheral-blood granulocytes, *J. Leukocyte Biol. 52*, 611−618.
11. Gleich, G. J., Loegering, D. A., Mann, K. G., and Maldonado, J. E. (1976) Comparative properties of the Charcot-Leyden crystal protein and the major basic protein from human eosinophils, *J. Clin. Invest. 57*, 633−640.
12. Otwinowski, Z., and Minor, W. (1997) Processing of X-ray diffraction data collected in oscillation mode, *Methods Enzymol. 276*, 307−326.
13. Brünger, A. T., Adams, P. D., Clore, G. M., DeLano, W. L., Gros, P., Grosse-Kunstleve, R. W., Jiang, J. S., Kuszewski, J., Nilges, M., Pannu, N. S., Read, R. J., Rice, L. M., Simonson, T., and Warren, G. L. (1998) Crystallography & NMR system: A new software suite for macromolecular structure determination, *Acta Crystallogr. D54*, 905−921.
14. Weis, W. I., Kahn, R., Fourme, R., Drickamer, K., and Hendrickson, W. A. (1991) Structure of the calcium-dependent lectin domain from a rat mannose-binding protein determined by MAD phasing, *Science 254*, 1608−1615.
15. Graves, B. J., Crowther, R. L., Chandran, C., Rumberger, J. M., Li, S., Huang, K. S., Presky, D. H., Familletti, P. C., Wolitzky, B. A., and Burns, D. K. (1994) Insight into E-selectin/ligand interaction from the crystal structure and mutagenesis of the lec/EGF domains, *Nature 367*, 532−538.
16. Hakansson, K., Lim, N. K., Hoppe, H. J., and Reid, B. M. (1999) Crystal structure of the trimeric α-helical coiled-coil and the lectin domains of human lung surfactant protein D, *Structure 7*, 255−264.
17. Boyington, J. C., Riaz, A. N., Patamawenu, A., Coligan, J. E., Brooks, A. G., and Sun, P. D. (1999) Structure of CD94 reveals a novel C-type lectin fold: Implications for the NK cell-associated CD94/NKG2 receptors, *Immunity 10*, 75−82.
18. Llera, A. S., Viedma, F., Sanchez-Madrid, F., and Tormo, J. (2000) Crystal structure of the C-type lectin-like domain from the human hematopoietic cell receptor CD69, *J. Biol. Chem. 276*, 7312−7319.
19. Natarajan, K., Sawicki, M. W., Margulies, D. H., and Mariuzza, R. A. (2000) Crystal structure of human CD69: A C-type lectin-like activation marker of hematopoetic cells, *Biochemistry 39*, 14779−14786.
20. Blundell, C. D., Mahoney, D. J., Almond, A., DeAngelis, P. L., Kahmann, J. D., Teriete, P., Pickford, A. R., Campbell, I. D., and Day, A. J. (2003) The link module from ovulation- and inflammation-associated protein TSG-6 changes conformation on hyaluronan binding, *J. Biol. Chem. 49*, 49261−49270.
21. Drickamer, K. (1993) Recognition of complex carbohydrates by Ca^{2+}-dependent animal lectins, *Biochem. Soc. Trans. 21*, 456−459.
22. Drickamer, K., and Taylor, M. E. (1993) Biology of animal lectins, *Annu. Rev. Cell Biol. 9*, 237−264.
23. Drickamer, K. (1992) Engineering galactose-binding activity into a C-type mannose-binding protein, *Nature 360*, 183−186.
24. Ng, K. K.-S., Drickamer, K., and Weis, W. I. (1996) Structural analysis of monosaccharide recognition by rat liver mannose-binding protein, *J. Biol. Chem. 271*, 663−674.
25. Weis, W. I., and Drickamer, K. (1996) Structural basis of lectin-carbohydrate recognition, *Annu. Rev. Biochem. 65*, 441−473.
26. Jacoby, D. B., Gleich, G. J., and Fryer, A. D. (1993) Human eosinophil major basic protein is an endogenous allosteric antagonist at the inhibitory muscarinic M2 receptor, *J. Clin. Invest. 91*, 1314−1318.
27. Rochester, C. L., Ackerman, S. J., Zheng, T., and Elias, J. A. (1996) Eosinophil-fibroblast interactions. Granule major basic protein interacts with IL-1 and transforming growth factor-β in the stimulation of lung fibroblast IL-6-type cytokine production, *J. Immunol. 156*, 4449−4456.
28. Trocme, S. D., and Hallberg, C. (1993) Heparin prevents eosinophil granule major basic-protein inhibition of corneal epithelial wound-healing in the rat, *Invest. Ophthalmol. Visual Sci. 34*, 1317.
29. Butterworth, A. E., Wassom, D. L., Gleich, G. J., Loegering, D. A., and David, J. R. (1979) Damage to schistosomula of *Schistosoma mansoni* induced directly by eosinophil major basic protein, *J. Immunol. 122*, 221−229.
30. Hamed, R. R., Maharem, T. M., and El-Guindy, A. S. (1997) Proteoglycans from adult worms of *Schistosoma haematobium*, *J. Helminthol. 71*, 151−160.
31. Frigas, E., Loegering, D. A., and Gleich, G. J. (1980) Cytotoxic effects of the guinea pig eosinophil major basic protein on tracheal epithelium, *Lab. Invest. 42*, 35−43.
32. Frigas, E., Loegering, D. A., Solley, G. O., Farrow, G. M., and Gleich, G. J. (1981) Elevated levels of the eosinophil granule major basic-protein in the sputum of patients with bronchial-asthma, *Mayo Clin. Proc. 56*, 345−353.
33. Flavahan, N. A., Slifman, N. R., Gleich, G. J., and Vanhoutte, P. M. (1988) Human eosinophil major basic protein causes hyper-reactivity of respiratory smooth muscle. Role of the epithelium, *Am. Rev. Respir. Dis. 138*, 685−688.
34. Furuyama, A., and Mochitate, K. (2000) Assembly of the exogenous extracellular matrix during basement membrane formation by alveolar epithelial cells *in vitro*, *J. Cell Sci. 113*, 859−868.
35. Li, D., Clark, C. C., and Myers, J. C. (2000) Basement membrane zone type XV collagen is a disulfide-bonded chondroitin sulfate proteoglycan in human tissue and cultured cells, *J. Biol. Chem. 275*, 22339−22347.
36. Esnouf, R. M. (1997) An extensively modified version of MOLSCRIPT that includes greatly enhanced coloring capabilities, *J. Mol. Graphics 15*, 132−134.
37. Barton, G. J. (1993) ALSCRIPT: A tool to format multiple alignments, *Protein Eng. 6*, 37−40.

BI051112B